Journal of
Nanophotonics

SPIEDigitalLibrary.org/jnp

Refractive index of laser active region based on InAs/InGaAs quantum dots

Nikita Yu Gordeev
Oleg I. Rumyantsev
Ivan G. Savenko
Alexey S. Payusov
Fedor I. Zubov
Mikhail V. Maximov
Alexey E. Zhukov

Refractive index of laser active region based on InAs/InGaAs quantum dots

Nikita Yu Gordeev,[a,b] Oleg I. Rumyantsev,[c] Ivan G. Savenko,[b,d,e] Alexey S. Payusov,[a,b] Fedor I. Zubov,[b] Mikhail V. Maximov,[a,b] and Alexey E. Zhukov[b]

[a]Ioffe Physical-Technical Institute, 26 Polytekhnicheskaya, St. Petersburg 194021, Russia
Gordeev@switch.ioffe.ru
[b]St. Petersburg Academic University, Nanotechnology Research and Education Centre, 8/3 Khlopina, St. Petersburg 194021, Russia
[c]Stanford University, Department of Applied Physics, 348 Via Pueblo Mall, Stanford, California 94305
[d]University of Iceland, Science Institute, Dunhagi-3, IS-107 Reykjavik, Iceland
[e]Nanyang Technological University, Division of Physics and Applied Physics, Singapore 637371, Singapore

Abstract. The effective refractive index of the active region of 1.3 μm edge-emitting tilted wave lasers based on InAs/InGaAs self-assembled quantum dots by the analysis of the far-field pattern is investigated. The obtained values of 3.485 and 3.487 in the operating lasers and in the cold waveguides, respectively, are well comparable with the refractive index of bulk InAs at corresponding wavelength. © *2013 Society of Photo-Optical Instrumentation Engineers (SPIE)* [DOI: 10.1117/1.JNP.7.073087]

Keywords: refractive index; self-assembled quantum dots; edge-emitting laser.

Paper 13031 received Apr. 21, 2013; revised manuscript received Jun. 14, 2013; accepted for publication Jun. 18, 2013; published online Jul. 18, 2013.

1 Introduction

The design of any optical cavities or waveguides to be used in optoelectronic devices requires adequate numerical simulations. One of the key parameters for such simulations is the refractive index of each cavity component. In some cases, correct values of refractive indexes are critical for the proper interpretation of the observed experimental data.[1,2] Refractive indexes of commonly used bulk semiconductors, such as GaAs and InGaAs, are quite well known and verified by a number of experiments and models.[3,4] There are experimental data and some comprehensive models of refractive indexes and related phenomena in quantum wells, widely used in optoelectronics. However, in literature, there is limited data on refractive indexes of quantum dot (QD) media. As often as not, a refractive index of QDs is adopted as the value for a bulk semiconductor with the same composition,[1] although the validity of doing so is doubtful. Strictly speaking, in the case of QDs, a refractive index can be considered only as an empirical parameter since a refractive index is a macroscopic measurable quantity. At the same time, optical properties of low-dimension materials strongly depend on the dielectric constant,[5] which is simply the square of the complex refractive index in nonmagnetic macroscopic media. In some cases, refractive index or dielectric constant profiles in waveguides can be reconstructed from measurements of spatial distributions, such as near-field or far-field patterns, of waveguide modes. Such methods have been successfully used for optical fibers[6] but are hardly applicable to reconstruct refractive index profiles of conventional edge-emitting semiconductor lasers. Their waveguide thicknesses are usually close to the diffraction limit so measurements of near-field patterns become a nontrivial task. Gaussian-like far-field patterns of these lasers are quite wide and are not to be used to determine modest changes of the waveguide refractive indexes.[7]

In this paper, we present our results on the reconstruction of the refractive index of InAs/GaAs QD active region from the analysis of the experimental far-field patterns measured for edge-emitting tilted wave lasers (TWL).

2 Waveguide Design

The concept of TWL (Ref. 8) is based on the existence of tilted modes originating in planar waveguides with thin cladding layers. The laser waveguide, schematically presented in Fig. 1, is based on two planar waveguides (1 and 3) coupled via a thin cladding layer (2) with lower refractive index. The active region is placed in the thin waveguide (1). The optical modes tunnel from this thin waveguide into the thick waveguide (3) and vice versa. The requirement for the thin waveguide is that it should support only one guided mode. The thick waveguide supports several modes but only one mode, effectively coupled with the thin waveguide, contributes to the lasing since it has the largest optical confinement factor. Thus, the lasing mode is a combined mode formed by the two coupled waveguides.

The most remarkable feature of the TWL is the mode spatial distribution schematically shown in Fig. 1. In the vertical far-field pattern, there are two major outer lobes and several lobes between them. A comprehensive theoretical analysis of TWL far-field patterns is presented in Ref. 9. The total number of lobes and their angular distribution mostly depends on the thick waveguide (3) thickness and its refractive index. At the same time, the waveguide coupling strength controls intensity redistribution between major and minor lobes. For example, in the case of stronger coupling, a larger fraction of the lasing mode is contained within the thick waveguide, which is expressed in the far-field pattern by the increased relative intensity of the two outer lobes. In the TWL waveguide, the coupling was found to be very sensitive to the changes in the thickness and the refractive index of the thin waveguide (1). Since the layer contains QDs, this gives an opportunity to reconstruct their refractive index from the analysis of the intensity redistribution between the lobes in the far-field pattern. It can be done by numerical fitting of the experimental far-field patterns when the unknown refractive index is used as a fitting parameter.

3 Growth and Processing

The QD structure used in this paper was grown by molecular beam epitaxy on a Si-doped (100) GaAs substrate. The active region contained 10 layers of self-assembled InAs QDs separated by 35-nm thick GaAs spacers. The active region was located in the middle of 0.95-μm thick GaAs waveguide layer. Composition and growth conditions of the active region were similar to the ones described earlier.[10] The structure had 1.5-μm thick p-$Al_{0.35}Ga_{0.65}As$ cladding layer and 200 nm p-GaAs contact layer. The lower part of the wafer was composed of 10.5-μm thick

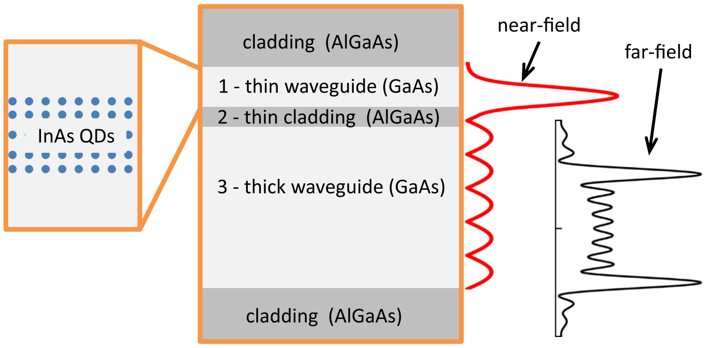

Fig. 1 Schematic cross-section of the edge-emitting laser with coupled cavities waveguide. Lasing mode profile (near-field) and far-field pattern are shown qualitatively.

n-GaAs coupled waveguide and 2-μm thick *n*-$Al_{0.35}Ga_{0.65}As$ reflecting layer. Two waveguides were coupled via 300-nm thick *n*-$Al_{0.35}Ga_{0.65}As$ layer. The TWL wafer was processed into 10 μm wide shallow-mesa ridge lasers by etching through the *p*-contact and partly through the *p*-cladding layer. The samples were mounted *p*-side down on copper heatsinks. To avoid any self-heating effects, the laser parameters were measured in pulsed mode at a fixed ambient temperature of 300 K.

4 Results and Discussion

The lasers emitted in the wavelength range of 1290 to 1305 nm depending on the cavity length. The lasers showed the threshold current density of 400 A/cm^2 and operated in the fundamental lateral mode that was confirmed by measurements of lateral far-field patterns. Transverse far-field patterns were measured at current densities just above the threshold. A typical experimental far-field is presented in Fig. 2(a) in solid line. This far-field pattern was fitted by a numerical simulation technique described below.

We simulated optical modes in the investigated waveguide by the software tool FIMMWAVE with embedded complex engine add-on.[11] The refractive indexes of GaAs and $Al_{0.35}Ga_{0.65}As$ layers used in the simulation were 3.413 and 3.227, respectively. They were calculated for the wavelength of 1300 nm from the empirical equations suggested by Afromowitz,[3] which reproduce within 0.004 the experimental data for moderately doped bulk GaAs and AlGaAs. It is important to note that to obtain 1.3 μm emission, the QDs were directly formed on a GaAs matrix by the deposition of 2.5 monolayers of InAs and then covered with a 5-nm thick $In_{0.15}Ga_{0.85}As$ layer.[10] In this case, the surface density of the QDs is about 3 to 5×10^{10} cm^{-2}. A form of QDs is usually assumed to be pyramidal though sometimes in numerical simulations even a simpler shape is used.[1] To avoid any ambiguity, we substituted in our simulation each layer of QDs by a layer with a homogenized refractive index n_{active}. This layer included InAs QDs, wetting layer, and InGaAs layer. Its total thickness of 6 nm corresponds to the amount of InAs and InGaAs from which the layer is formed. We used n_{active} as the only parameter for the far-field fitting. Thicknesses of the waveguide layers were verified by scanning electron microscopy technique. Normalized simulated far-field pattern is presented in Fig. 2(a) in dotted line. The lasing mode is TE_8 mode. It fits the experimental curve with a very good accuracy. Two zoomed-in parts of the experimental far-field pattern and two simulated curves with n_{active} of 3.483 and 3.487 are presented in Fig. 2(b). It is clearly seen that minor changes in fitting parameter n_{active} redistribute intensity between major and minor lobes. The experimental curve is located between two simulated curves. From these values, we can estimate the refractive index of QD active region as 3.485 with the accuracy of 0.004. The latter is simply the difference between 3.487 and 3.483. This accuracy matches with the accuracy of refractive indexes of GaAs and $Al_{0.35}Ga_{0.65}As$ layers calculated by Afromowitz's equations. [3] The refractive indexes

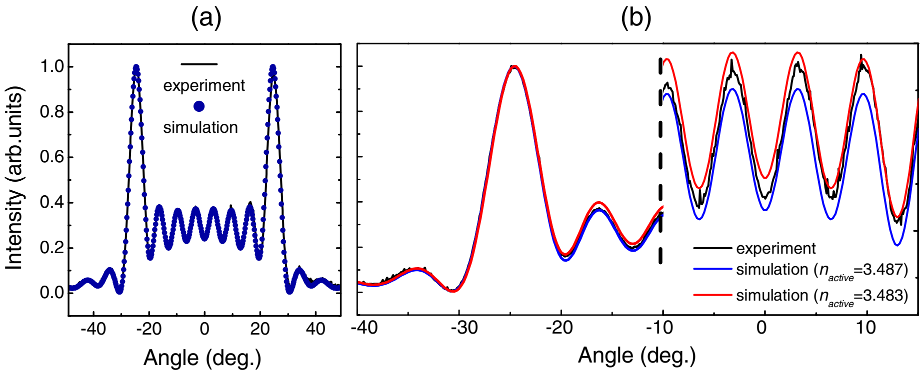

Fig. 2 Normalized experimental and simulated far-field patterns of the TWL based on QDs (pumping current density $J = 1.25 \times J_{\text{threshold}}$): (a) entire far-field patterns and (b) zoomed-in parts of the far-field patterns (scale factor in the right part is larger).

determined for different laser samples lie in the same error range. The value of n_{active} is applicable for the wavelength range of 1290 to 1305 nm where the investigated lasers emitted.

We note that carrier-induced refractive index variation was neglected in the numerical simulation of TWL waveguides. Material differential refractive index $\mathrm{d}n/\mathrm{d}N$, where N is the carrier density, is usually negative, so cold QD active regions have higher refractive indexes than n_{active} determined from fitting of the far-field patterns. This variation Δn_{active} can be estimated as $\Delta n_{\text{active}} = (\mathrm{d}n/\mathrm{d}N) \times N$, where N in its turn is calculated from a simplified equation $N = (J \times \tau)/(q \times d)$, where J is the threshold current density, τ is the carrier lifetime, q is the electronic charge, and d is the total thickness of the QD layers. We assumed that the recombination takes place only in the active region via the QD ground state and that the Fermi levels pin at and above the threshold. We used the following parameters: differential refractive index $\mathrm{d}n/\mathrm{d}N = 0.7 \times 10^{-20}\ \mathrm{cm}^{-2}$ (Ref. 12), carrier lifetime $\tau = 0.78$ ns (Ref. 12), $d = 10 \times 6$ nm, and $J = 400\ \mathrm{A/cm}^2$. The carrier-induced refractive index variation was found to be $\approx 2.3 \times 10^{-3}$ by substituting all the parameters into the equation for Δn_{active}. Thus, in the cold laser waveguide n_{active} is slightly higher, namely, 3.487.

The obtained refractive index of the QD active region n_{active} is comparable with the refractive index of bulk InAs at corresponding wavelength[4] and higher than the refractive index that would have been expected for the layer containing a significant amount of $\mathrm{In}_{0.15}\mathrm{Ga}_{0.85}\mathrm{As}$. This qualitatively indicates that the dielectric constant of InAs QDs is higher than that of bulk InAs which can be attributed to the size dependence of dielectric constants of low-dimension materials. However, an analysis of this is beyond the scope of this paper.

5 Conclusion

Specific transverse far-fields of TWL allowed determining the refractive index of the QD active region by numerical fitting of the experimental far-field patterns. It was found that in the operating lasers, the active region based on InGaAs self-assembled QDs emitting at 1.3 μm has the refractive index as high as 3.485, whereas in the cold active region the index was estimated to be slightly higher, namely, 3.487. The obtained values can be used for modeling optoelectronic devices which have similar QD active regions.

Acknowledgments

This work was supported in different parts by the EC's Seventh Framework Programme under grant agreement no. 224211 VISIT, and by Russia's Federal Program "Scientific and Educational Manpower for Innovative Russia" (Project No. 8692). The authors are grateful to Innolume GmbH (Dortmund, Germany) for the laser wafer growth. The contributions of the different authors are as follows: MVM designed the laser wafer, AEZ participated in the laser wafer growth, FIZ processed the laser wafer, ASP and OIR measured the laser diodes, OIR and IGS simulated the laser parameters, and NYG supervised this project and was responsible for writing the manuscript.

References

1. B. D. Jones et al., "Splitting and lasing of whispering gallery modes in quantum dot micropillars," *Opt. Express* **18**(21), 22578–22592 (2010), http://dx.doi.org/10.1364/OE.18.022578.
2. O. Qasaimeh et al., "Linear and quadratic electro-optic coefficients of self-organized $\mathrm{In}_{0.4}\mathrm{Ga}_{0.6}\mathrm{As/GaAs}$ quantum dots," *Appl. Phys. Lett.* **72**(11), 1275–1277 (1998), http://dx.doi.org/10.1063/1.121049.
3. M. A. Afromowitz, "Refractive index of Ga1−xAlxAs," *Solid State Commun.* **15**(1), 59–63 (1974), http://dx.doi.org/10.1016/0038-1098(74)90014-3.
4. S. Adachi, "Optical dispersion relations for GaP, GaAs, GaSb, InP, InAs, InSb, $\mathrm{Al}_x\mathrm{Ga}_{1-x}\mathrm{As}$, and $\mathrm{In}_{1-x}\mathrm{Ga}_x\mathrm{As}_y\mathrm{P}_{1-y}$," *J. Appl. Phys.* **66**(12), 6030–6040 (1989), http://dx.doi.org/10.1063/1.343580.

5. M. Tian, M. Li, and J. C. Li, "Effect of size on dielectric constant for low dimension materials," *Physica B* **406**(3), 541–544 (2011), http://dx.doi.org/10.1016/j.physb.2010.11.034.
6. W. S. Tsai, S. Y. Ting, and P. K. Wei, "Refractive index profiling of an optical waveguide from the determination of the effective index with measured differential fields," *Opt. Express* **20**(24), 26766–26777 (2012), http://dx.doi.org/10.1364/OE.20.026766.
7. D. Botez, "Design considerations and analytical approximations for high continuous wave power, broad-waveguide diode lasers," *Appl. Phys. Lett.***74**(21), 3102–3104 (1999), http://dx.doi.org/10.1063/1.124075.
8. N. Y. Gordeev et al., "Edge-emitting InGaAs/GaAs laser with high temperature stability of wavelength and threshold current," *Semicond. Sci. Technol.* **25**(4), 045003 (2010), http://dx.doi.org/10.1088/0268-1242/25/4/045003.
9. V. Shchukin et al., "Tilted wave lasers: a way to high brightness sources of light," *IEEE J. Quantum Electron.* **47**(7), 1014–1027 (2011), http://dx.doi.org/10.1109/JQE.2011.2132116.
10. A. R. Kovsh et al., "InAs/InGaAs/GaAs quantum dot lasers of 1.3 μm range with enhanced optical gain," *J. Cryst. Growth* **251**(1–4), 729–736 (2003), http://dx.doi.org/10.1016/S0022-0248(02)02506-X.
11. Photon Design, "FIMMWAVE. Introduction," http://www.photond.com/products/fimmwave.htm (11 June 2013).
12. A. A. Ukhanov et al., "Comparison of the carrier induced refractive index, gain, and linewidth enhancement factor in quantum dot and quantum well lasers," *Appl. Phys. Lett.* **84**(7), 1058–1060 (2004), http://dx.doi.org/10.1063/1.1647688.

Nikita Yu Gordeev graduated from St. Petersburg State Electrical Engineering University, Russia, in 1993 and received a PhD from Ioffe Physical Technical Institute, St. Petersburg, Russia, in 1998. In the same year, he joined Center of Nanoheterostructure Physics, Ioffe Institute. He has authored and co-authored more than 170 journal and conference papers. He is a principal researcher in a number of national and international projects. His main research interests lie in the field of III–V optoelectronics: edge emitting lasers based on quantum well and QDs, microcavity, and photonic crystals devices, coherence properties of semiconductor devices.

Oleg I. Rumyantsev received a BS degree from St. Petersburg Polytechnical University in 2009 and an MS from St. Petersburg Academic University of the Russian Academy of Sciences in 2011 specializing in physics and technology of nanostructures. His research interest was focused on developing efficient semiconductor quantum well and QD lasers for optoelectronic and high-brightness applications. He is currently pursuing a PhD degree at Stanford University.

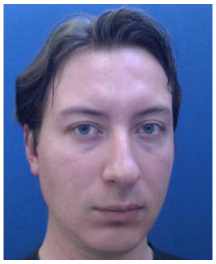

Ivan G. Savenko is a theoretical physicist. He works in the University of Iceland, Reykjavik, and St. Petersburg Academic University, Russia. Besides, Ivan is a research assistant in the Nanyang Technological University, Singapore. He completed his BSc in the field of micro- and nano-electronics in St. Petersburg Polytechnical University, Russia, in 2008 and an MSc in St. Petersburg Academic University in 2010. Ivan's current research fields include photonic crystals, mesoscopic transport and cavity polaritons, condensation phenomena in solid state physics, zero-, two-, and three-dimensional objects in microcavities, terahertz sources in semiconductors, and surface plasmons.

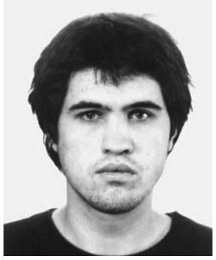

Alexey S. Payusov received an MSc in 2007 from St. Petersburg State University of Information Technologies Mechanics, and Optics, Russia. In 2011, he received a PhD degree in semiconductor physics from St. Petersburg Academic University, Nanotechnology Research and Education Centre of the Russian Academy of Sciences, Russia, where he currently works as a researcher. His current research interests include physics of nanostructures, development of high-power high-brightness semiconductor lasers and vertical-cavity surface emitting lasers for telecommunication.

Fedor I. Zubov received an MSc degree in technical physics from St. Petersburg State Polytechnical University, Russia, in 2008. Until 2010, he was with R&D Company Phystex, Vaals, Netherlands, as a research fellow, where he worked on creation of radiation sources for extreme ultraviolet lithography. He is currently working toward a PhD degree at St. Petersburg Academic University, Russia. His current research interests include semiconductor QDs and edge-emitting laser diodes.

Mikhail V. Maximov has worked at Ioffe Physico-Technical Institute since 1989. He received Candidate of Science (PhD) and Doctor of Science (habilitation) degrees in physics and mathematics from Ioffe Institute in 1995 and 2010, respectively. He has co-authored more than 400 papers. In 2000, he was awarded by the Alexander von Humboldt Research Fellowship. He is a team leader in the number of international and Russian projects. His main interests are related to development and optical studies of novel optoelectronic devices based on self-organized QDs: edge emitting and vertical cavity surface emitting lasers, microlasers, microcavity, and photonic crystals devices.

Alexey E. Zhukov graduated as an optical engineer from Leningrad Electrical Engineering Institute in 1992 and joined Ioffe Physical-Technical Institute, St. Petersburg, Russia. He received a PhD degree in 1996 and the Doctor of Science degree in 2002 from Ioffe Institute. He is a correspondent-member of the Russian Academy of Sciences (RAS). He has authored and co-authored more than 600 publications. His current interests are in low-dimensional structures, diode lasers, QDs, and AlGaInAs heterostructures. He is currently a pro-rector and a head of a lab at St. Petersburg Academic University of RAS.